FUNDAMENTAL ASPECTS OF NEUTRON SPECTROSCOPY

S.I. Sukhoruchkin, Z.N. Soroko, M.S. Sukhoruchkina

Petersburg Nuclear Physics Institute NRC "Kurchatov Institute" 188300 Gatchina

1 Introduction

Neutron resonance spectroscopy provides data on a large number of highly excited nuclear states. This information can be used to check nuclear microscopic models, including the Nonrelativistic Constituent Quark Model (NRCQM), which, according to R. Feynman, is successful [1]. Its extension, the Electron-based Constituent Quirk Model (ECQM), combines the properties of hadrons and leptons with the universal character of the influence of a physical condensate (vacuum) [2]. ECQM model provides a possibility to estimate the discreteness in particle masses and energies of nuclear states, as well as to explain nonstatistical effects in the neutron resonance positions and spacing distributions. The systematic character of these effects is due to the fundamental dynamics, which is manifested itself in the CODATA relations for the nucleon masses. Empirically, it was found that the QED correction $\alpha/2\pi$ coincides with the ratios between the parameters of NRCQM (M_q=441 MeV), single-particle structure ($m_e = \varepsilon_\circ/2$) and fine and superfine structures in neutron resonances [3]. In Tables 1 and 2 and in Figs. 1 and 2, the main empirical observations used in the development of the ECQM model are presented [4-7].

Table 1. Intervals in particle masses (MeV), noted by G. Wick, R.Sternheimer and P. Kropotkin.

| Author	$Part._{top}$	Mass	$Part._{bottom}$	Mass	Interval	Mass	n	$n \times \delta$	diff.
Wick	K°	497.62	muon	106.16	$K^\circ - \mu$	391.45	48	392.45	1.00
Wick	neutron	939.57	η	547.86	$n - \eta$	391.71	48	392.45	0.71
Sternheimer	η	547.86	muon	106.16	$\eta - \mu$	441.70	54	441.50	0.20
Sternheimer	neutron	939.57	K°	497.61	$n - K^\circ$	441.96	54	441.50	0.46
Kropotkin-CQM	Ξ	1342 /3	M_q		M_q	441	54	441.50	
Sternheimer	Σ°	1383.7	neutron	939.57	$\Sigma^\circ - n$	441.1	54	441.50	0.4
Sternheimer	$K^{*\pm}$	891.55	ω	782.65	$K^{*\pm} - \omega$	109.01	13	106.29	2.72
	$K^{*\circ}$	895.81	ω	782.65	$K^{*\circ} - \omega$	113.16	13	106.29	
Fig. 2, top	K_3^*	1776(7)	$K^{*\circ}$	895.81	$K_3^* - K^*$	880(7)	108	883.0	3(7)
Fig. 2, bottom	ω_3	1667(4)	ω	782.65	$\omega_3 - \omega$	884(4)	108	883.0	1(4)
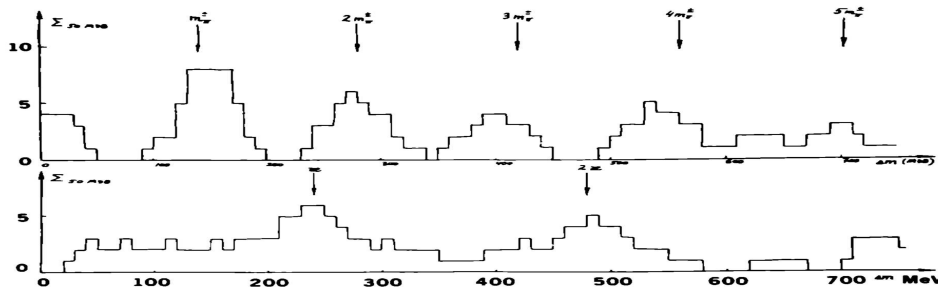
Figure 1: Ideohistograms of distribution of differences between masses of baryon singlets (top, ΔM with the averaging interval 25 MeV). Arrows mark the period 140 MeV=$m_{\pi^\pm}$.

Y. Nambu was the first who noticed that the mass of a pion is a common parameter of the particle mass spectrum [4]. The representation of baryon singlet masses as an integer pion mass is shown in Fig. 2 as a straight line passing through the hyperons Λ, Ξ, Ω and the charmed quark $m_c \approx 9m_\pi$ (dark circle in Fig 2). In the previous report at this conference it was shown that the neutron mass m_n deviates from the integer m_n by 161 keV=$m_\pi(\alpha/2\pi)$. The factor $\alpha/2\pi = 115.96 \cdot 10^{-5}$, which is very close to the ratio $1/(32 \times 27)115.74 \times 10^{-5}$, was found empirically [3] as the ratio between the stable mass/energy intervals shown in lines 3-6 of Table 2.

The initial mass of the baryon constituent quark in NRCQM $M_q = m_e(\alpha/2\pi)^{-1}$ was introduced by P. Kropotkin (under the name "gammon") long before NRCQM [8,9]. With the stable interval 391 MeV=$m_\omega/2 = 3f_\pi$, introduced by G. Wick (Table 1 [7]), it corresponds to the discreteness in particle masses with periods 130-140-147 MeV (close to f_π, m_π, Fig. 1) and nucleon mass evolution from $3M_q$ to $m_\omega + M_q/3$=932 MeV (Fig. 2).

Table 2. Comparison of the parameter $\alpha/2\pi$=115.96·10^{-5} with the anomalous magnetic moment of the electron $\Delta\mu_e/\mu_e$ [8-10] (top line), parity nonconservation parameter $\eta_\pm/2$ (observation by J. Bernstein [8-10], second line) and with the ratios between the mass/energy values introduced in [3] (lines No 4-6) and other parameters mentioned in literature (below).

No.	Parameter	Components or the ratio	Value $\times 10^5$
	$\Delta\mu_e/\mu_e$	=$\alpha/2\pi$-0.328 α^2/π^2	115.965
	$\eta_{+-}/2$ [10]	2.232(11)$\times 10^{-3}$/2	112(1)
	$2\delta m_\pi - 2m_e$	(81652(10) keV)/(16m_e=δ)	132(12)
1	$\delta m_\mu/m_\mu$	(23$\times$9m_e-m_μ)/m_μ	112.1
2	m_μ/M_Z	m_μ/M_Z=91182(2) MeV	115.87(1)
3	$\delta m_n/m_\pi$	(k$\times m_e$-m_n)/m_π=161.649 keV/m_π	115.86
4	$\varepsilon''/\varepsilon'$	1.35(2) eV/1.16(1) keV	116(3)
5	$\varepsilon'/\varepsilon_o$	1.16(1) keV/ε_o=1022 keV	114(1)
6	$(\varepsilon_o/6)/\Delta M\Delta$		116.02
7	$(\Delta M_\Delta = M_q/3)/M_{H°}$	147 MeV/125 GeV	118
8	$\delta/\delta°$	$\delta° = 16M_Z/(L = 207)$=7.048 GeV	116.0
9	m_d/m_b, [10]	m_d=4.78(9) MeV/ m_b=4.18(3) GeV	114
10	m_u/m_c, [10]	m_u=2.2(5) MeV/ m_c=1275(25) MeV	173(40)
11	Sb, D(187 eV)/161 keV	(373 eV/2=187 eV)/160 keV	114
12	Pd, D(1497 eV)/1293 keV		115.7
13	Hf, D(1501 eV)/δm_N	^{172,176}Hf $E^*(0^+)$=1293 keV=δm_N	116.1
14	Os, D(1198 eV)/2m_e	^{178,180}Os $E^*(0^+)$=1023 keV=2m_e	117
14	Pd,Cd D(1501 eV)/δm_N	^{97}Pd $E^*(2^+)$=1293 keV	
15	D(1585 eV)/8m_e/3[12, 13]	^{even}Sn $E^*(0^+)$=4m_e	
16	Cd-Xe D(1437 eV)	^{112}Cd $E^*(0^+)$ 1222 keV	117
17	D(1723 eV) [12,13]	^{110}Cd $E^*(0^+)$ 1473 keV	116
18	D(2007 eV) [12,13]	^{108}Cd $E^*(0^+)$ 1721 keV	117
19	Te D(2375 eV)/4m_e [20]	^{even}Te $E^*(0^+)$=4m_e	116
20	N=90 D(793 eV)/4m_e/3	$E^*(0^+)$=682 keV=(4/3)m_e	
21	D=1.19 keV/ε_o [14]	ΣE^*=ε_o=1022(2) keV)	117
22	D=1188 keV/ε_o [15]	ΣE^*=ε_o=1022(2) keV)	117
23	ε'=1.276 keV, Fig. 4	$\varepsilon' \cdot (A/A + 1) : \varepsilon_o$	119
24	^{241,242,243}Pu, Figs. 8-10	D=99(2) eV)/2($E^*(2^+)$=42.5 keV)	117
25	^{239}U	D=1506 eV/1295 keV	116

Parameters of the ECQM model $M_q^\omega = m_\omega/2 = 3f_\pi = 48\delta{=}391\,\mathrm{MeV}$ and $M_q = m_\Xi/3 = 3\Delta M_\Delta = 54\delta{=}441\,\mathrm{MeV}$ are boxed in Table 1. Important relations between these parameters and lepton masses are shown at the top of Fig. 2, where a coincidence of the difference between the masses of the ω_3 meson and ω meson (boxed in bottom line of Table 1) and the corresponding difference between the masses of K^* and K_3^* mesons to the value of $2M_q{=}882\,\mathrm{MeV}$, shown by three parallel lines in Fig. 2 (and the difference between them of $1\,\mathrm{MeV}$, boxed in bottom line of Table 1) is observed. The evolution of the nucleon mass from $M_q \approx m_\Xi/3$ ends at the mass of the nucleon in the nuclear media $m \approx m_N$-$8\,\mathrm{MeV}{=}932\,\mathrm{MeV}{=}m_\omega + \Delta M_\Delta$ [21,22]. So, we see that the components of the ratio, found by P. Kropotkin, $m_e/M_q = \varepsilon_\circ/3\Delta M_\Delta = \alpha/2\pi$ (line in Table 2) correspond to several clearly interpreted parameters.
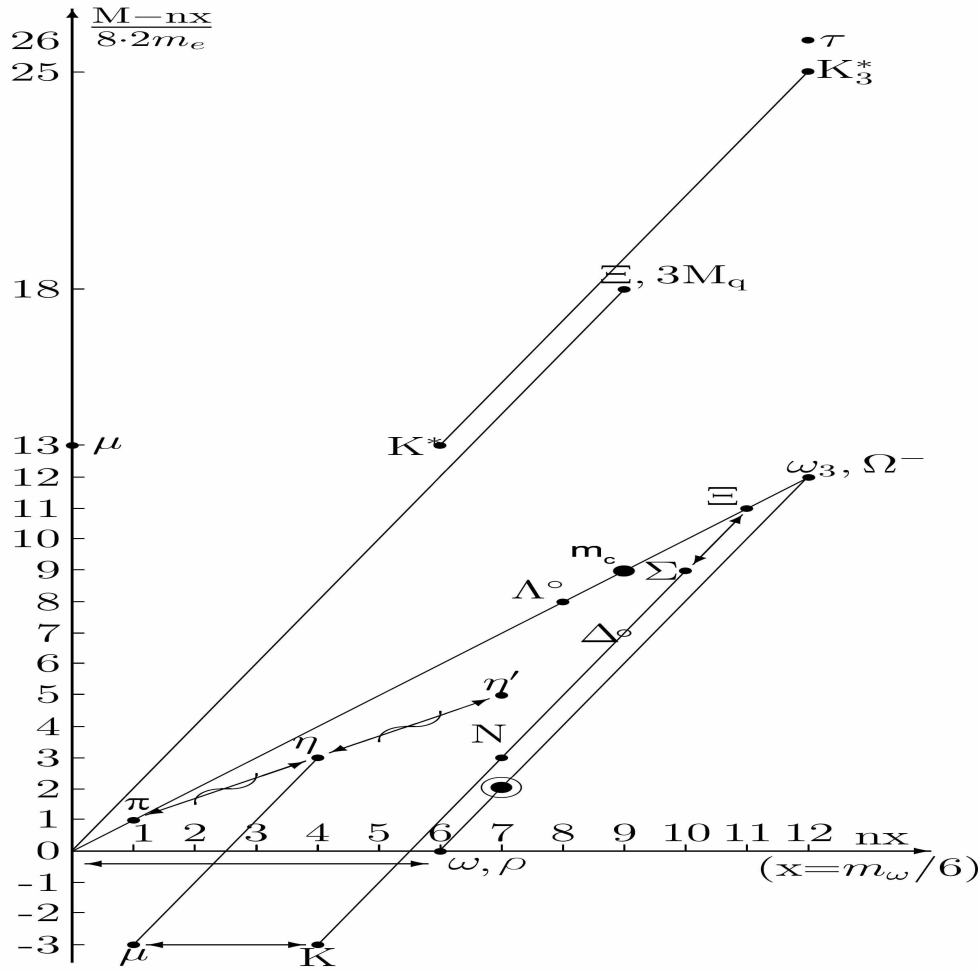

Figure 2: The evolution of the baryon mass from $3M_q$ to the nucleon mass M_N is shown in a two-dimensional presentation: the values in the horizontal direction are given in units of $16 \cdot 16 m_e = f_\pi{=}130.7\,\mathrm{MeV}$, the remainders M_i-$\mathrm{n}(16 \cdot 16 m_e)$ are plotted along the vertical axis in $16 m_e$. The nucleon mass in a nuclear medium (circled point) is close to the sum $\Delta M_\Delta + 6f_\pi$. Three different slopes correspond to three pion parameters: $f_\pi = 16\delta$, $m_{\pi^\pm} = 17\delta$ and $\Delta M_\Delta = 18\delta$. The mass of the τ lepton is close to $2m_\mu + 2m_\omega$.

2 Fine structure in neutron resonances

Using a special table BNL-325 [14] where ten strong resonances in each nucleus are presented, the grouping was found at $E_n=2\varepsilon'$ and $4\varepsilon'$ with the fine structure parameter $\varepsilon'=1.188\,\text{eV}$. This common parameter was determined from the correlations noticed by M. Ohkubo [15] in the positions of resonances in the compound nuclei ^{82}Br, ^{124}Sb, and ^{141}Ce. Other stable intervals in spasing of neutron resonances were observed in [16-20].

The strong neutron resonance position E'_n (after recoil correction) is the difference between the E^* state with a relatively simple wave function structure and S_n. The value $18.8\,\text{keV}=2\delta'$ (found as a maximum in the distribution of positions of relatively strong neutron resonances of light N-even nuclei Z≤28, Fig. 30, top) corresponds to the 4th maximum in spacing distribution of neutron resonances in the near-magic ^{61}Ni (Fig. 30). 6 out of 14 values $E_n=E^*-S_n$, forming a maximum at 18.8 keV, were obtained from Z-magic nuclei (Z=20, 28). Parameters $\delta'=19\,\text{keV}/2=9.5\,\text{keV}$ and $\varepsilon'=\delta'/8=1.2\,\text{keV}$ [21] are given in Table 3 (bottom).
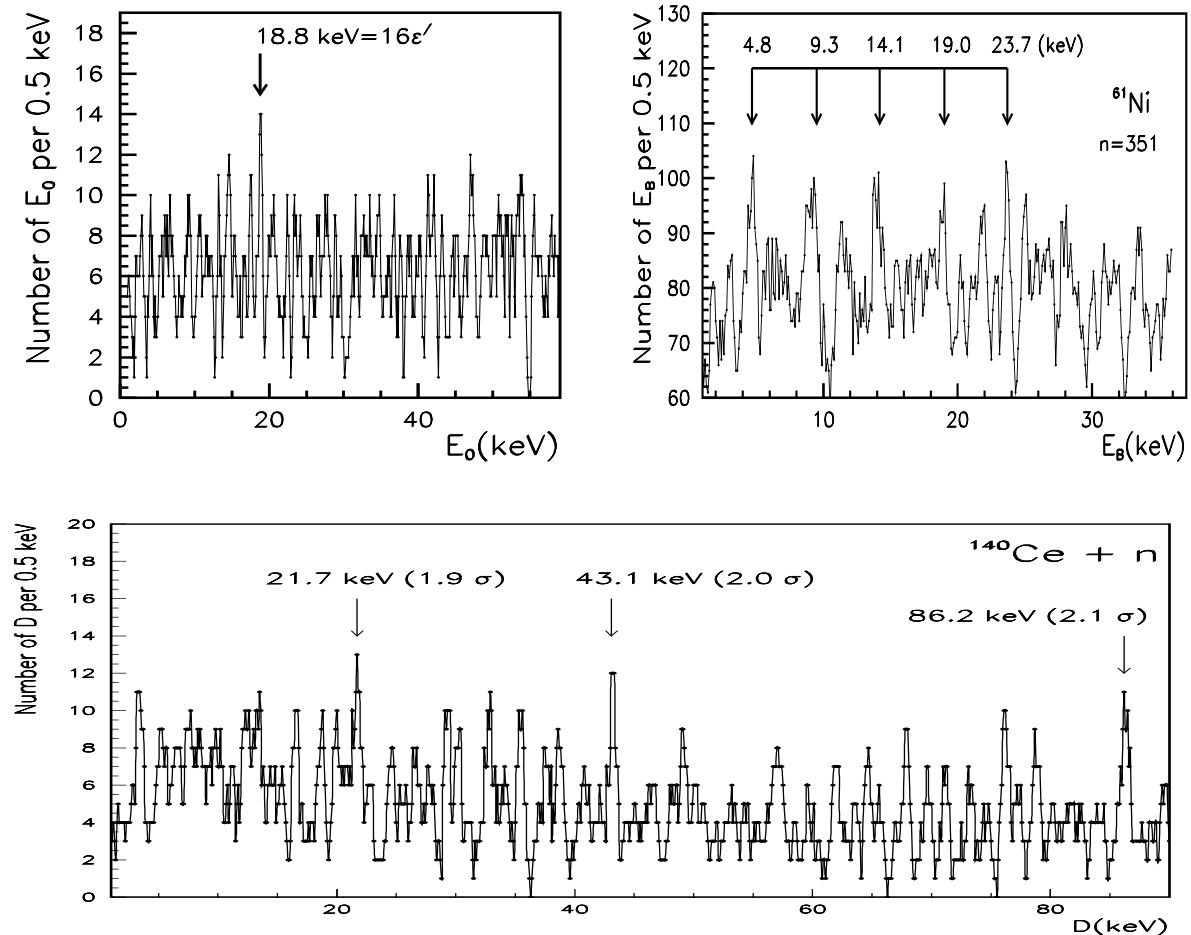

Figure 3: *Top:* Distribution of resonance positions in all N-even light nuclei. *Center:* Distribution of neutron resonance spacing in the target ^{60}Ni (the number of resonances n=351). *Bottom:* Spacing distribution of ^{141}Ce neutron resonances (period 21.7 keV).

Table 3. Comparison of positions and spacings in light and near-magic nuclei with integer values of the fine structure parameter $\varepsilon' = \delta'/8 = 1.188\,\text{keV}$. *Top:* Positions E'_n of strong neutron resonances in light and magic nuclei and periodicity in the spacing distributions in resonances ^{61}Ni (top right). *Center:* Values E_n in nuclei with N=83=82+1, maxima in spacing distributions ^{141}Ce. *Bottom left:* The positions of strong neutron resonances in isotopes with Z=35-39 are compared with the integer of the period ε'=1.188 keV=9.505 keV/8, found in the positions of strong resonances in Z=57-59, N=83 nuclei (center). *Bottom right:* Excitation energies E^* of ^{143}Ce. Boxed are values ε'=1.188 keV=9.505 keV/8, δ', $2\delta'$ and $(9/4)\delta'$ discussed in the text.

Nucl.	Ca-Ni	^{61}Ni	^{61}Ni	^{61}Ni	^{61}Ni	^{61}Ni Fig. 3, center
l_n	$l_n=0$	D(keV)				
E_n	18.8	4.8	9.3	14.1	19.0	24.7
$k(\varepsilon')$	16	4	8	12	16	20
$k \times \varepsilon'$	19.0	4.8	9.6	14.4	19.0	24.7

Nucl.	^{141}Ce	^{141}Ce	^{142}Pr	^{141}Ce	^{141}Ce	^{141}Ce Fig. 3, bottom
J_i^π	$1/2^+$	$1/2^+$	$(5/2^-)$			
Γ_n^o,meV	660*	3060*	160	D	D	D
E_n	9.573	21.570	9.598	21.7	43.1	86.2
E^*,E'_n	$\boxed{9.505}$	$\boxed{21.418}$	$\boxed{9.530}$			
$k(8\varepsilon')$	1	9/4	1	9/4	9/2	9
$k \times 8\varepsilon'$	$\boxed{9.504}$	21.384	$\boxed{9.504}$	21.4	42.5	85

Nucl.	^{140}La	^{80}Br	^{82}Br	^{86}Rb	^{143}Ce	$J_o^\pi=3/2^-$
J_i^π	3^+	$l_n=0$	$l_n=0$	$l_n=0$	$7/2^-$	$5/2^-$
Γ_n^o,meV	54	72.0	120	159	E^*	E^*
E_n	1.179	1.201	1.209	2.398		
E^*,E'_n	$\boxed{1.170}$	$\boxed{1.186}$	$\boxed{1.194}$	2.370	$\boxed{18.9}$	42.3
$k(8\varepsilon')$	1/8	1/8	1/8	2/8	2	9/2
$k \times 8\varepsilon'$	1.188	1.188	1.188	2.376	19.0	42.77

It was noticed [15] that in ^{141}Ce, the positions of the two strongest resonances (marked with * and ** in Table 2) are in the ratio 9:4=2.25 (2.253, in fact). The same ratio (2.237) exists between the energies of low-lying excitations ^{143}Ce (Table 2, center). The triplet of these closely spaced levels (the next E^* is at 633 keV) is the result of the residual interaction between three valence neutrons. One could notice a 1:2 ratio of the values E'_n in ^{141}Ce to E^* in ^{143}Ce (ratio 0.505). E'_n of strong s-resonances in some other N=83 nuclei are related to these E'_n. For example, E'_n in ^{142}Pr is close to that of ^{141}Ce (marked as $8\varepsilon'$=8×1.188 keV), while E'_n in ^{140}La is close to ε' (see Table 2).

In the near-magic ^{145}Sm (N=83), the position of the p-wave resonance with the largest Γ_n^1 is close to ε', while the stable spacing of its s-wave and p-wave resonances (n=143, D=3689 eV and n=62, D=2485 eV, see Fig. 3) are close to $3\varepsilon'$=3564 eV and $2\varepsilon'$=2376 eV.

Stable intervals D=595 eV=$\varepsilon'/2$ and D=294 eV=$\varepsilon'/4$ were found in resonances ^{134}Cs and ^{128}I.

It was found that the clustering of strong resonances in ^{82}Br [15] has a small (0,03) occasional probability of grouping. It is shown in Table 3 that E'_n of the strongest resonances in ^{80}Br, ^{82}Br and ^{86}Rb are close to ε' and $2\varepsilon'$. In ^{182}Ta, E'_n of the two strongest s-resonances are ε' and $\varepsilon'/2$.

In this work, we show that in the D-distributions of neutron resonances in ^{145}Sm (for orbital momenta L=0 and 1, Fig. 2, top and bottom), the maxima are located exactly at $3\varepsilon'$ and $2\varepsilon'$.

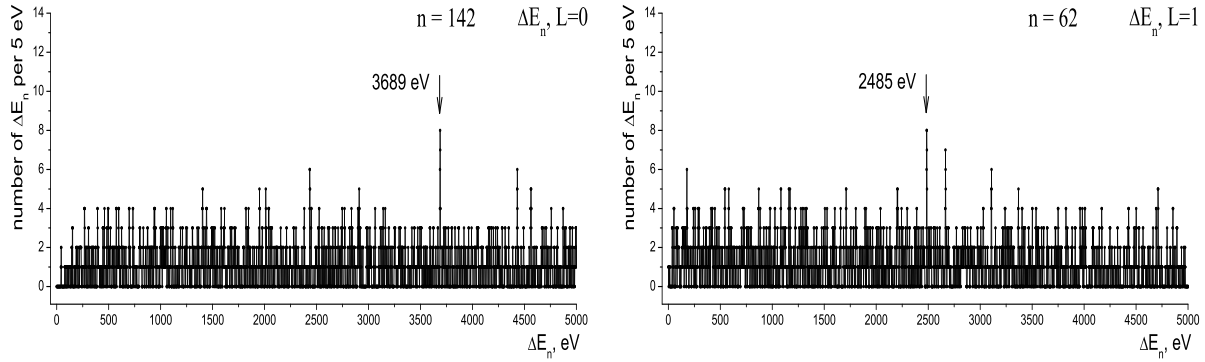Figure 4: Spacing distributions of neutron resonances in ^{145}Sm (for orbital momenta L=0 and L=1 with maxima at $3\varepsilon'$ and $2\varepsilon'$ ($3689\,\mathrm{eV}/2485\,\mathrm{eV}{=}1.48{\approx}3/2$, $\varepsilon'{=}1.226\,\mathrm{keV}$).
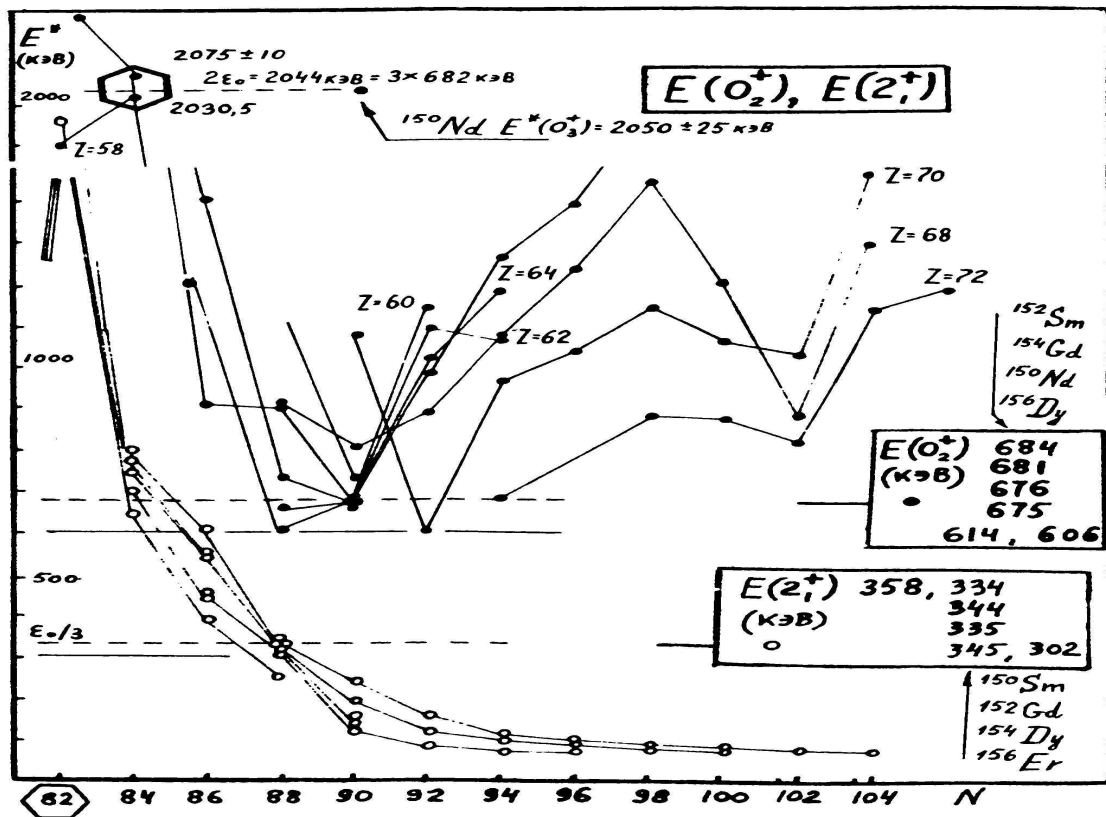

Figure 5: Bunching of energies of 0^+ excitations of nuclei with the number of neutrons 90 (filled $2f_{7/2}$ neutron subshell) at a value of $2/3\varepsilon_o{=}682\,\mathrm{keV}$. The values of the excitations are indicated by dark circles and are connected by lines for each serial number with the corresponding Z on the right side. In the same nuclei (neutrons number N = 62-104), the first excitations (2^+) are shown in the figure with light circles. When the number of neutrons is 88 = 90-2, the grouping of the values of 2^+ excitations occurs at a value of $340\,\mathrm{keV}{=}\varepsilon_o/3$. The $\varepsilon_o/3$, $(2/3)\varepsilon_o/3$ and $2\varepsilon_o$ energy levels are shown with dashed lines. The top of the figure shows the closeness to $2\varepsilon_o$ of the energies of the nuclei levels ^{132}Ce (N = 84 = 82 + 2) and ^{150}Nd (N=90).

3 Superfine structure in neutron resonances

The superfine structure in the position and spacing distribution of neutron resonances was found in different nuclei by many authors [15-20]. Selecting the reduced widths of neutron resonance, the positions and the spacing distributions shown in Fig. 6 were obtained. There is a proximity of the maximum in positions of resonances at 5 eV to four intervals $\varepsilon'' = 5.5\,\text{eV}/4 = 1.34\,\text{eV}$, observed in sum spacing distribution [3]. For example, in the niobium, the position of the strongest resonance ($\Gamma_n^o = 218\,\text{meV}$) at 5.78 eV (close to $5.5\,\text{eV} = \delta''/2 = 11\,\text{eV}/2$) is four times the position of the resonance at $1.34\,\text{eV} = \varepsilon''$.

An example of superfine structure in the spacing distribution of strong neutron resonances (corresponding to highly excited states with a relatively simple wave function structure) was found in ^{238}Np. Selecting the reduced widths of neutron resonance larger than 50 and 100 meV, we obtained the spacing distributions shown in Fig. 7. From the proximity of the doublet of resonance positions at 1.32 eV and 1.48 eV to $\varepsilon'' = 5.5\,\text{eV}/4 = 1.38\,\text{eV}$ and the position of the strongest resonance ($\Gamma_n^o = 218\,\text{meV}$) at 5.78 eV to 5.5 eV, we see that stable intervals 4.1 eV, 5.6 eV and 16.4 eV are close to $3\varepsilon''$, $4\varepsilon''$ and $12\varepsilon''$.
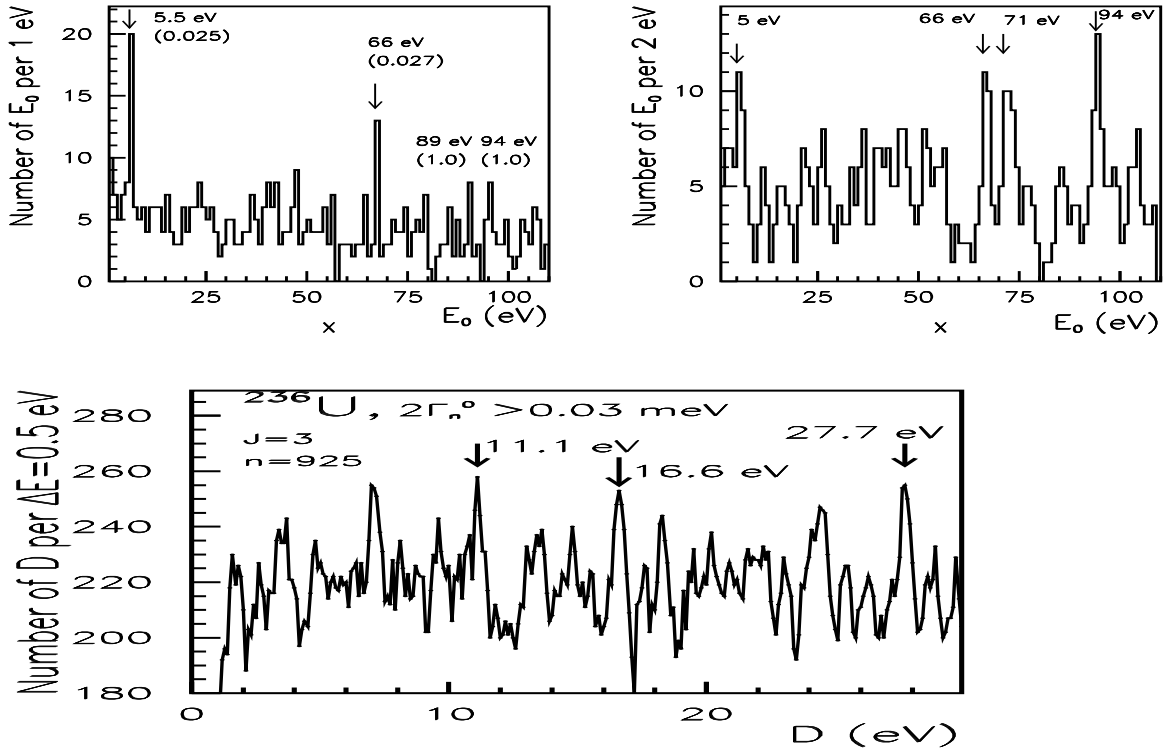

Figure 6: *Top*: Distribution of neutron resonance positions (1970s) by selection of one resonance (max Γ_n^o) in the interval 10 eV and 100 eV. *Bottom*: Spacing distribution of $J=3$ ^{235}U resonances. Integers $k=1$, 2, 3, 5, 12, 13 and 17 of the period of $5.5\,\text{eV} = \delta''/2$ are marked.

In Nb (Fig. 7), positions of the doublet of resonances at 1.32 eV and 1.48 eV are close to the maximum (at 1.1 eV) in the spacing distribution (top), while in the distributions for more strong resonances maxima are observed at $4.1\,\text{eV} = 3\varepsilon_o$, $5.6\,\text{eV} = 4\varepsilon_o$ and $16.4\,\text{eV} = 12\varepsilon_o$, as well as at $54.8\,\text{eV} = 5\delta' = 40\varepsilon_o$ and 87.8 eV, close to $88\,\text{eV} = 8\delta' = 64\varepsilon_o$.
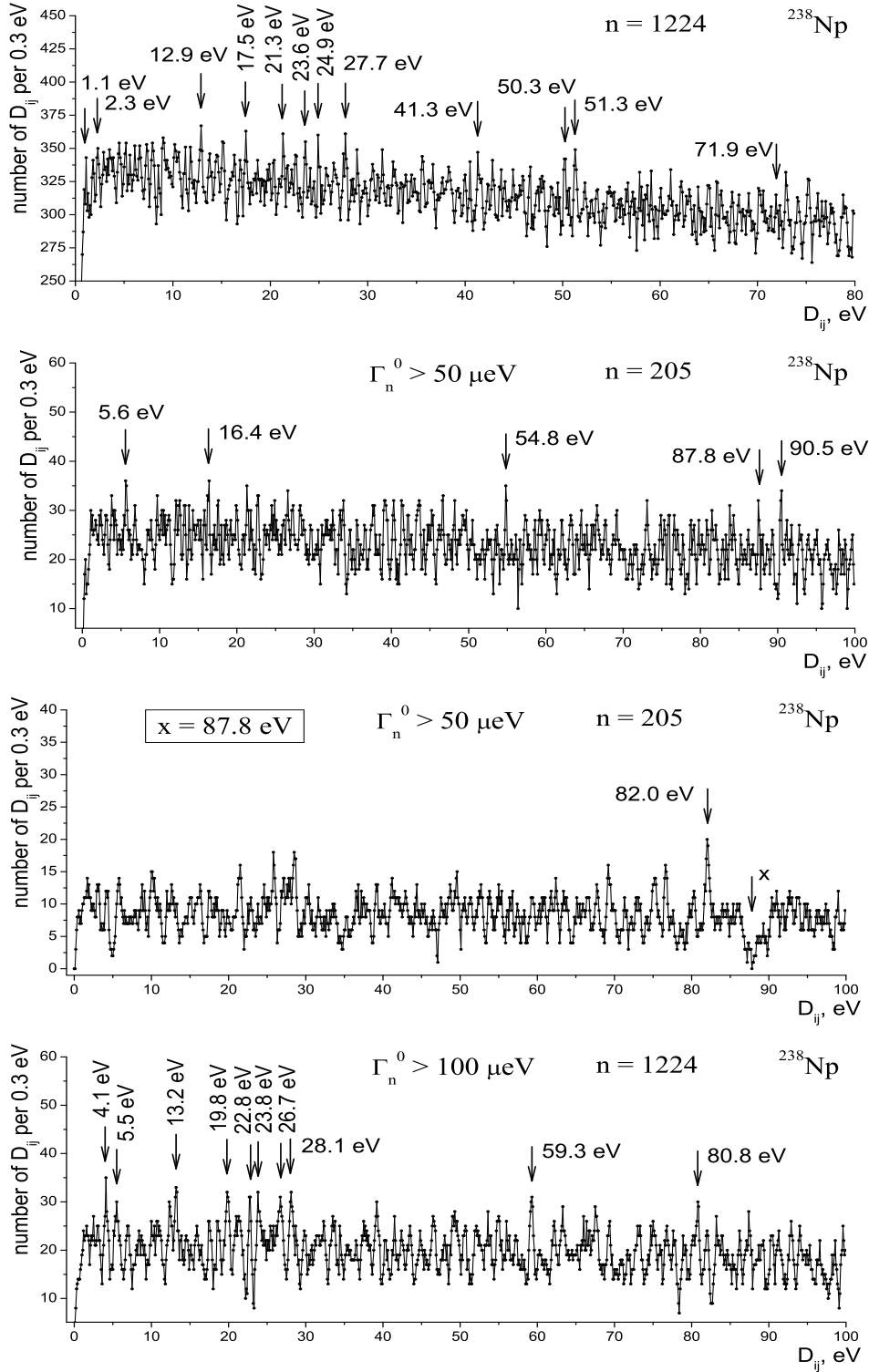
Figure 7: *Top*: Total spacing distribution of all resonances in ^{238}Np. *2nd line*: Spacing distribution of resonances in ^{238}Np with $\Gamma_n^\circ \geq 50\mu$eV. *Center*: Adjacent spacing distribution of resonances in ^{238}Np with $\Gamma_n^\circ \geq 50\mu$eV for the fixed interval x=87.8 eV. *Bottom*: Spacing distribution of resonances in ^{238}Np with $\Gamma_n^\circ \geq 100\mu$eV.

The stable interval $D=99\,\mathrm{eV}=9\delta''$ was observed in Pu isotopes, in which stable excitation $43\,\mathrm{keV}=6\times6\delta'$ is well known and is shown in Fig. 8 ,top (maximum in the spacing distribution of all 188 low-lying states). The correspondence between intervals 99 eV (see Figs. 9, 10) and 43 keV are shown in the bottom lines Table 2, where similar correspondence between levels of the neighbour nucleus ^{239}U is shown (considered in the work that follows).
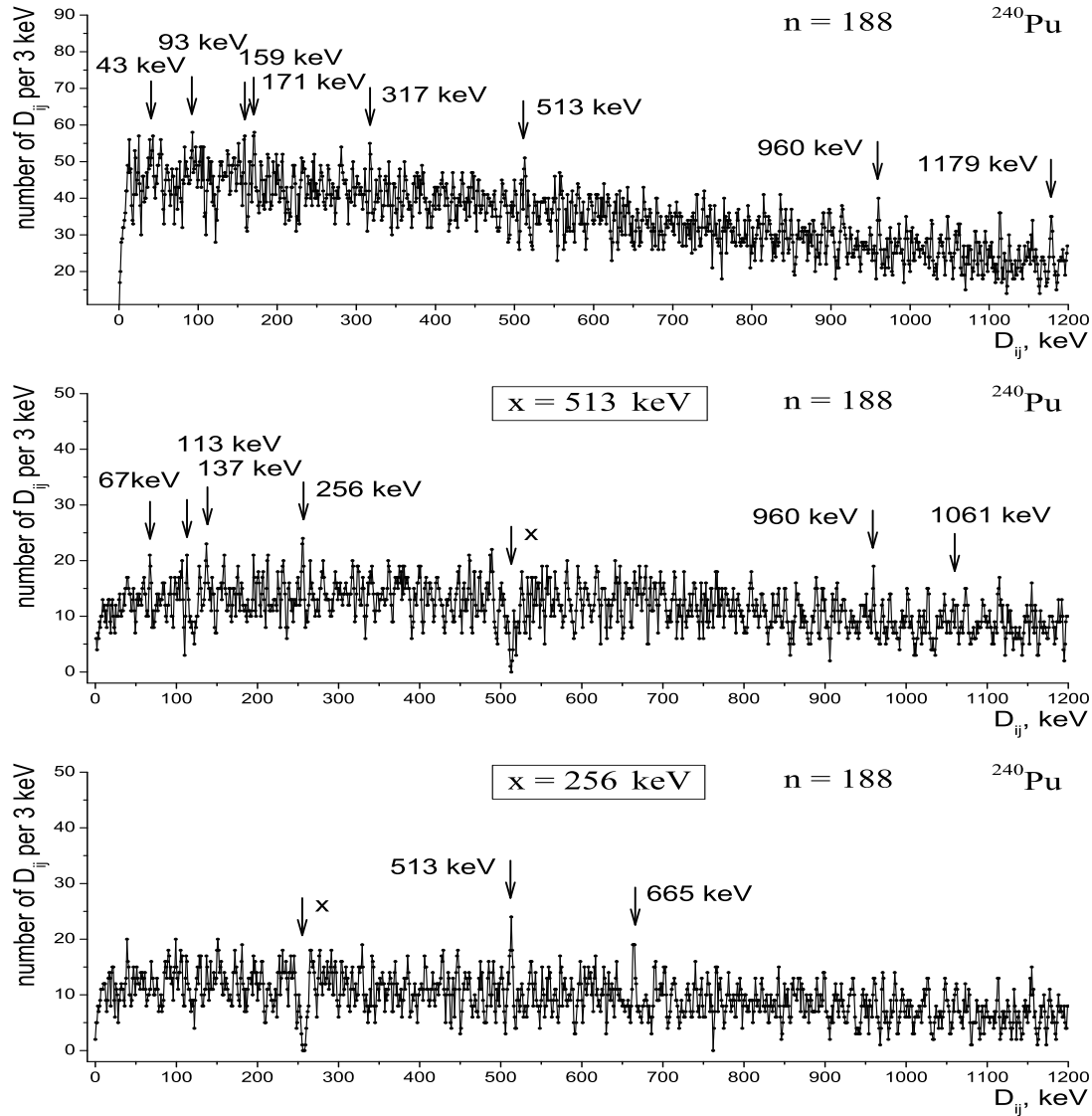

Figure 8: *Top*: Total spacing distribution of low-level ^{240}Pu states with the maximum at 43 keV corresponding to stable excitations in many heavy nuclei. *Center and bottom*: Distribution of intervals adjacent to x=513 keV and 256 keV.

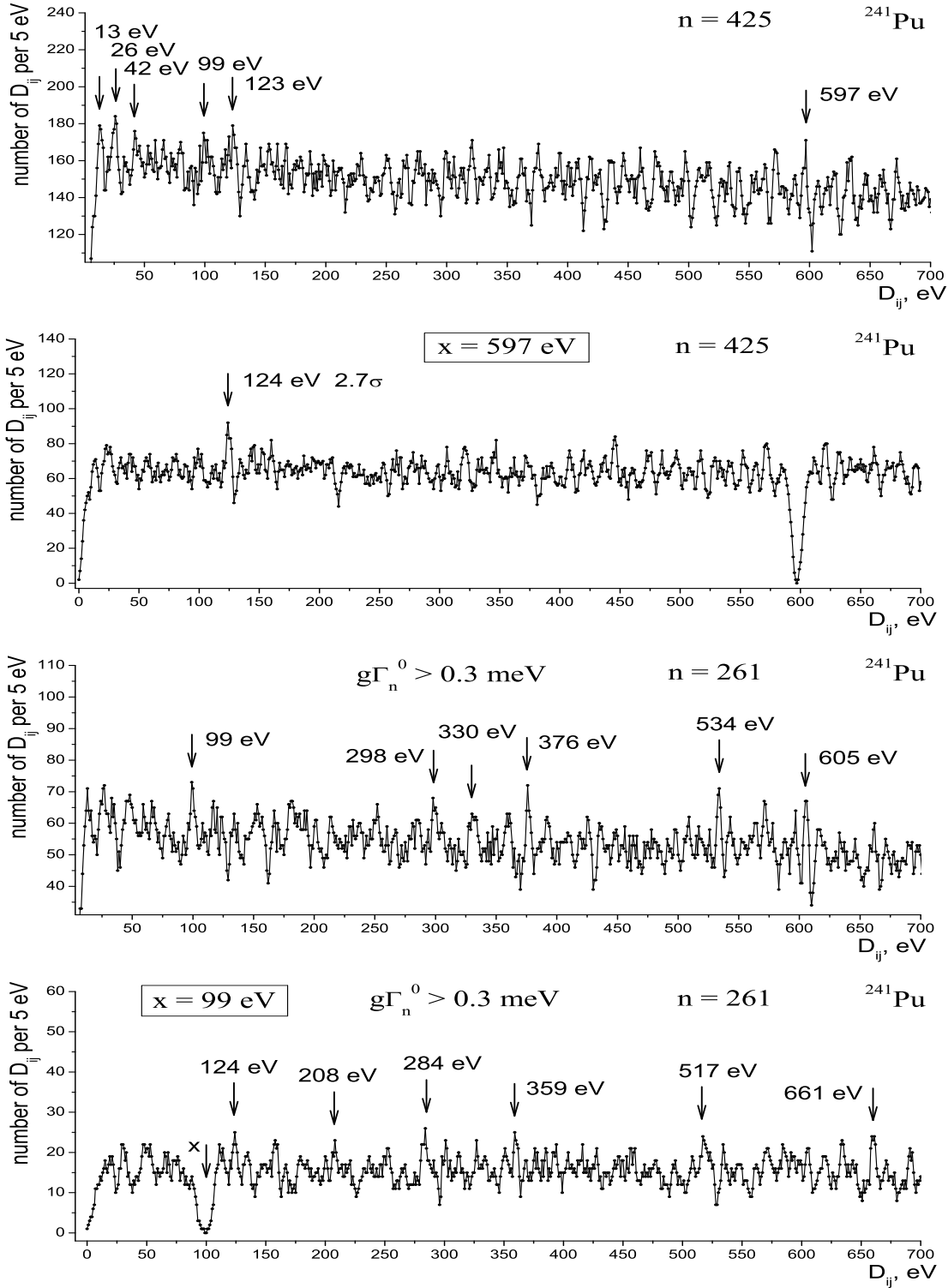Figure 9: *Top*: Total spacing distribution of all resonances in ^{241}Pu with the maximum at $99\,\mathrm{eV}{=}9\delta'$. *2nd line*: Resonance spacing distribution in ^{241}Pu adjacent to $x{=}597\,\mathrm{keV}$. *Center*: Resonance spacing distribution in ^{241}Pu with $\mathrm{g}\Gamma_n^o \geq 0.3\,\mathrm{meV}$ with the maximum at $99\,\mathrm{eV}{=}9\delta''$. *Bottom*: Resonance spacing distribution in ^{241}Pu with $\mathrm{g}\Gamma_n^o \geq 0.3\,\mathrm{meV}$ adjacent to $x{=}99\,\mathrm{eV}$.
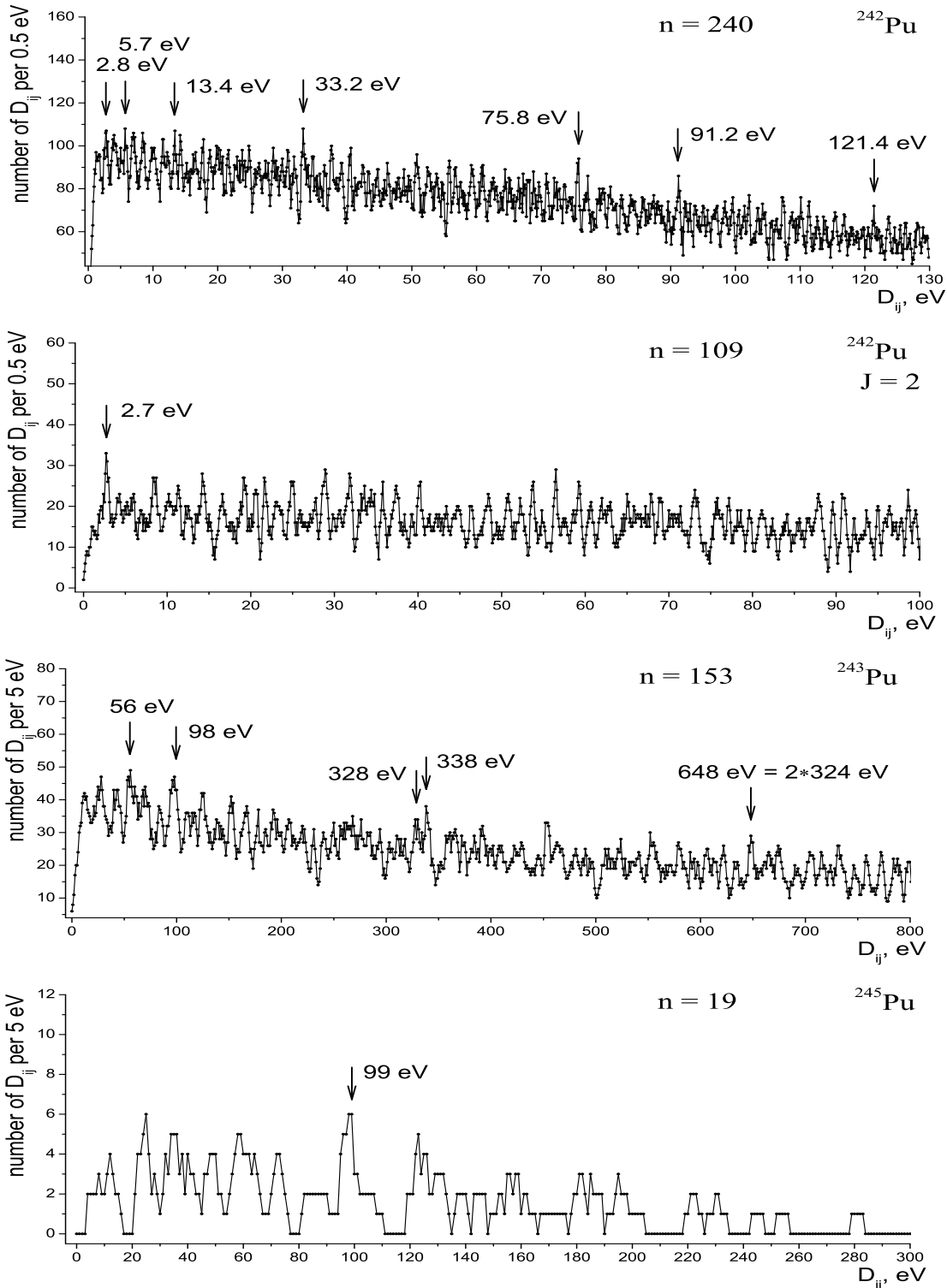
Figure 10: *Top*: Total spacing distribution of all resonances in ^{242}Pu. *2nd line*: Total spacing distribution of all resonances in ^{242}Pu for J=2 with the maximum at 2.7 eV. *Center*: Total spacing distribution of all resonances in ^{243}Pu with the maximum at $98\,\mathrm{eV}=9\delta''$. *Bottom*: Total spacing distribution of all resonances in ^{245}Pu with the maximum at $99\,\mathrm{eV}=9\delta''$.

4 Conclusions

The recently presented analysis of fine and superfine structures in the spacing of neutron resonances (all data from [25], see also introductions there) confirmed the results obtained in [3,8,9,11-13,20-24] that the coincidence of the ratio between the parameters of these structures demonstrate the important role of the influence of physical condensate (vacuum). Empirically established accurately known CODATA relations [21,22]:

$$m_n = 115 \cdot 16 m_e - m_e - \delta m_N/8 \quad m_p = 115 \cdot 16 m_e - m_e - 9\delta m_N/8 \qquad (1)$$

show two symmetry motivated factors $16 : 1 = \delta : m_e$ and $3 : 1 = m_e : 170\,\mathrm{keV}$, where $170\,\mathrm{keV} = m_e/3$ and $161\,\mathrm{keV} = \delta m_N/8$ are related to the real fundamental mass splitting.

A near coincidence of the QED radiative correction $\alpha/2\pi = 115.96 \cdot 10^{-5}$ to the ratio $1/(32 \times 27) = 115.74 \cdot 10^{-5}$ allows to suggest that the nuclear data, including neutron resonance data, can indirectly verify the presence of fundamental relations observed in the particle mass spectrum, for example, the lepton ratio as a reflection of the mass discreteness and symmetry.

References

1. F. Close, CERN Courier **53** (2017) No 3, p. 31.
2. V. Belokurov, D. Shirkov, *Theory of Particle Interactions.* AIP, 1991.
3. S.I. Sukhoruchkin, *Statistical Properties of Nuclei.* Pl. Press, 1972, p. 215.
4. Y. Nambu, Progr. Theor. Phys. **7** (1952) 595.
5. P. Kropotkin, *Field and Matter*, Moscow Univ., 1971, p. 106.
6. P. Kropotkin, Doklady Ac. Nauk URSS **206** (1972) 304.
7. R. Sternheimer, Phys. Rev. **136** (1964) 1364; **170** (1968) 1267.
8. S.I. Sukhoruchkin *et al.*, Proc. ISINN-27, JINR E3-2020-10, pp. 40, 54.
9. S.I. Sukhoruchkin *et al.*, Proc. ISINN-9, JINR E3-2001-192, pp. 314, 342, 351.
10. P.A. Zyla *et al.*, Progr. Theor. Exp. Phys. **2020** (2020) 083C01.
11. S.I. Sukhoruchkin *et al.*, Proc. ISINN-3, Dubna, 1995. JINR E3-95-37, pp.182, 330.
12. S.I. Sukhoruchkin, Proc. ISINN-2, JINR E3-94-192, pp. 234, 326.
13. Z. Soroko *et al.*, Proc. ISINN-5, JINR E3-97-213, p. 370.
14. S. Mughabghab, *Neutron Cross Sections*, **1**, part B, p. A-1, 1984.
15. M. Ohkubo *et al.*, J. Nucl. Sci. Techn. **18(10)** (1981) 745; JAERI-M-93-012, 1993.
16. F.N. Belyaev, S.P. Borovlev, Yad. Fiz. **27** (1978) 289.
17. G. Rohr, Proc. 8th Symp. Capt. Gamma-Rays, Fribourg, 1993. W.Sc., 1994, p. 626.
18. G. Rohr, in: *Low Energy Nuclear Dynamics*, p. 130. World Scientific, 1995.
19. K. Ideno, J. Phys. Soc. Jpn. **37** (1974) 581 .
20. Z.N. Soroko *et al.*, Proc. ISINN-7, Dubna, 1999. JINR E3-99-212, p. 313.
21. S.I. Sukhoruchkin, Nucl. Part. Phys. Proc. **312-317** (2021) 185.
22. S.I. Sukhoruchkin, Nucl. Part. Phys. Proc. (in press).
23. S.I. Sukhoruchkin *et al.*, Proc. ISINN-8, Dubna. JINR E3-2000-192, pp. 420, 428.
24. S.I. Sukhoruchkin *et al.*, Proc. ISINN-10, Dubna. JINR E3-2003-10, pp. 290, 299.
25. S.I. Sukhoruchkin, Z.N. Soroko, in: *Neutron resonance parameters*, Landoldt-Börnstein New Series, vols. **I/24**, **I/26A**. Springer, 2009, 2015. Ed. H. Schopper.